

Fabrication of Nanorod Light Emitting Diode by Ni Nano-cluster and Enhanced Extraction Efficiency

Mumta Hena Mustary¹, Volodymyr V. Lysak¹

¹*School of Semiconductor and Chemical Engineering, Semiconductor Physics Research Center, Chonbuk National University, Jeonju 561-756, Republic of Korea*

Abstract: We demonstrate InGaN/GaN nanorod light emitting diode (LED) with significantly enhanced emission efficiency. Our nanorod LED has been fabricated by top down approach using self-assembled Ni nano-clusters as an etching mask during ICP etching. Nanorod LED has nowadays become very interesting to the researchers because of its strain relaxation effect that induced in InGaN/GaN MQWs. Our nanorod LED structure showed 9 nm (54meV) blue shift in peak emission wavelength compared to conventional LED which confirms the strain relaxation in InGaN/GaN MQWs and 2.8 times PL intensity enhancement which reflects the enhancement of internal quantum efficiency (IQE). Furthermore, extraction efficiency has been calculated using FDTD simulation. Our simulation results showed extraction efficiency up to 80% for nanorod LED.

Keywords: Light emitting diode, Nano-cluster, Nanorod, Strain relaxation, Internal quantum efficiency, Light extraction efficiency, Finite Difference Time Domain (FDTD).

I. Introduction

GaN based blue light emitting diodes (LEDs) have attracted considerable interest in the development of optoelectronic devices [1, 2]. Especially, InGaN/GaN multiple quantum well (MQW) are being used as the active layers for optical devices such as light-emitting diodes (LEDs) and laser diodes (LDs). In the last two decades, tremendous efforts have been spent on the development of LEDs, leading to commercialization. However, InGaN/GaN materials still have inherent difficulties and further improvement in optical performance is still essential to meet the requirements for replacement of conventional lighting source. One of the fundamental limits results from internal electrical fields in InGaN/GaN MQWs induced by the large lattice mismatch, leading to a significant reduction in optical efficiency. This is becoming even worse when the LEDs are moving toward longer wavelength such as green spectral region [3–6] generating so-called “green gap” phenomenon. Another factor is the high dislocation density (10^9 – 10^{11} cm⁻²) of the epitaxial layer grown on the heterosubstrate, leading to a debasing influence on the device performance [7]. InGaN/GaN nanorods have been considered the most promising technique to reduce piezoelectric polarization by exposing the nonpolar planes (m- or a-planes) [8-10]. Furthermore, the increased effective emission area obtained by stretching the length of GaN nanorods can also potentially enhance the light output power [11]. For a more enlarged emission area, highly ordered nanostructure arrays are of importance for mask templates in wafer scales. For GaN-based nanoscale structures, so far, the GaN nanorods have been produced by various fabrication methods, such as growth of InGaN/GaN multiple quantum nanocolumns/nanorods on Si substrate by radiofrequency (RF) plasma-assisted molecular-beam epitaxy [12] or growth of single-crystal GaN nanorods by hybrid vapor-phase epitaxy [13], synthesis using carbon nanotubes as templates [14], inductively coupled plasma-reactive ion etching (ICP-RIE) without masks [15] or via e-beam patterned [16] nanorods, each with a relatively complicated process. To simplify the patterning process, it is possible to produce self-assembled nickel (Ni) nano-cluster by choosing the correct Ni layer thickness, annealing time and annealing temperature on top of the LED surface. In addition, recent advances in fabricating nanoscale InGaN/GaN structures using bottom-up approaches have enabled spectral tunability from blue to even red in the visible spectrum range by controlling the size of nanorods (NRs) or the current density [17–18].

In this paper, we have fabricated InGaN/GaN nanorod LEDs by top-down approach. Self-assembled Ni nano-cluster was used as an etching mask during ICP dry etching process. Our nanorod LED showed large blue shift of PL intensity peak due to strain relaxation effects and significant improvement of photoluminescence (PL) intensity which reflect the enhancement of internal quantum efficiency. Furthermore, extraction efficiency has been calculated using FDTD simulation software.

II. Fabrication Procedure

For nanorod LED fabrication, first self-assembled Ni nano-cluster is adopted. Fabrication of self-assembled Ni nanomasks [19], which is not only simple to control but also cheap in formation compared to the holographic lithography technique [20]. For Ni cluster formation first we deposited Ni film on the LED surface followed by rapid thermal annealing (RTA).

A typical RTA operating system consists of three phases: (1) rapid heating to the desired operating temperature, (2) the processing phase, in which temperature is held constant and (3) rapid cooling to ambient conditions.

An energy balance on the wafer in the RTA chamber gives

$$\rho C \frac{\partial T}{\partial t} = q_k + q_c + q_r \quad (1)$$

Where ρ , C and T are the wafer density, specific heat and temperature, t is the time and q_k , q_c and q_r are the heat transfer rates by conduction, convection and radiation, respectively.

First Ni film thickness, RTA temperature and time under N_2 ambient were optimized for getting perfect Ni nano-clusters surface. Ni film of different thicknesses was first deposited by E-beam evaporation on LEDs surfaces and then rapid thermal annealed at different temperature and time. Perfect Ni cluster can formed by depositing 3nm thick Ni film followed by rapid thermal annealed at $850^{\circ}C$ for 30s. Top view SEM image of Ni cluster surface is shown in Fig.1.

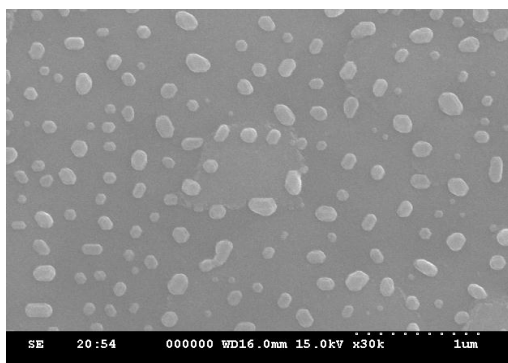


Fig. 1. SEM images of 3nm thick Ni film after RTA at $850^{\circ}C$, N_2 ambient for 30s.

After formation of perfect Ni clusters, this surface was used as an etching mask during ICP dry etching process. Nanorod InGaN/GaN MQW was fabricated by using ICP etching under gas flow of Cl_2 (20sccm) and BCl_3 (10sccm) for 160s. The cross sectional and top view SEM images are shown in Figure 2(a) and 2(b) respectively. The average diameter of our nanorod was ranging from 200-300 nm and height of the rod was about $\sim 435nm$. After that residual Ni nano-cluster was removed by dipping the samples into aqua regia ($3HCl:HNO_3$).

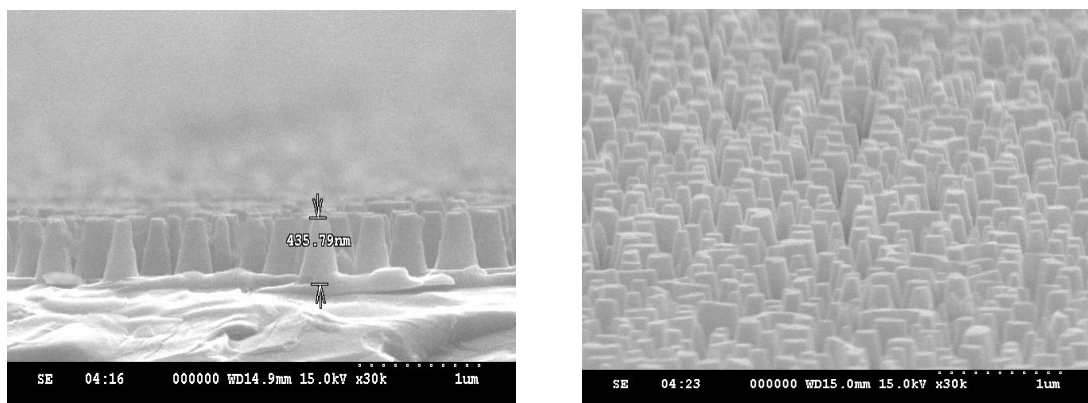


Fig. 2 (a) The cross sectional SEM image of Nanorod LED **(b)** Top view of Nanorod LED surface.

III. Results and Discussions

3.1 Enhanced PL intensity

Our nanorod LED fabricated using the above approach exhibit significant improvement in photoluminescence (PL) intensity. As shown in Fig. 3 PL intensity enhanced significantly in case of our nanorod LED. There is about 2.8 times enhancement in light intensity observed in nanorod LED compared to planar structure. The enhanced PL intensity can be mainly attributed to a significant increase in internal

quantum efficiency (IQE). In addition, such nanorod structure provides a larger surface area and more pathways which can lead to a reduction in total internal reflection (TIR) effect, thus increasing light extraction efficiency. Moreover, the emission peak from the nanorod sample shows a clear blue-shift of about 9 nm (54meV) compared to the planar LED sample. It is well-known that there exists strong strain-induced piezoelectric fields exerted across InGaN/ GaN MQWs, causing so-called quantum confined Stark effect (QCSE) and thus generating a red-shift in emission peak which is the main drawback for green to red emission LED fabrication. The optical pumping induced blue-shift in emission peak which occurs to our InGaN/GaN nanorod structure confirms that the strain has been relaxed as a result of fabrication into nanorod structure.

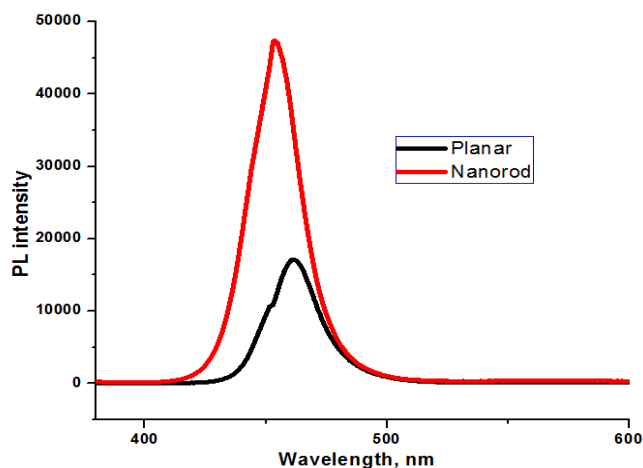


Fig. 3. Photoluminescence (PL) intensity of planar and nanorod LED.

3.2 FDTD Simulation model and Enhanced Extraction Efficiency

After observing the Strain relaxation and enhanced PL intensity experimentally, we have used FDTD simulation software to optimize light extraction efficiency (LEE). FDTD simulation is based on Maxwell's curl equations exist to simulate light extraction. The FDTD method offers many significant advantages for simulation, including a full-wave solution, finely controlled accuracy via the size of the simulation grid and steps, and accounting of all optical phenomenons of reflection, refraction, and diffraction. Fig. 4 shows the schematic cross sectional view of nanorod LED simulation structure.

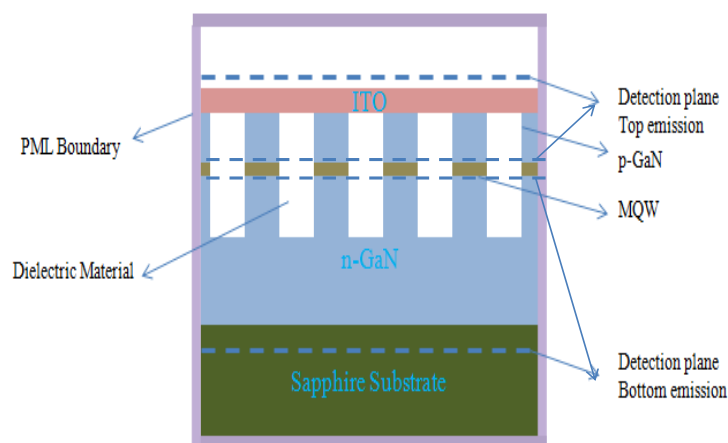


Fig 4. Schematic cross sectional view of nanorod LED simulation model.

In the simulation, the thickness of the n-GaN layer is fixed at 2200 nm, the refractive indices of the sapphire substrate, the GaN layers, and the InGaN MQW layers are 1.78, 2.5, and 2.55, respectively. The radius of the rods was varied. The refractive index of the transparent conductive layer (TCL) material is chosen to be 2.0 which is the refractive index of Indium-tin-oxide (ITO).

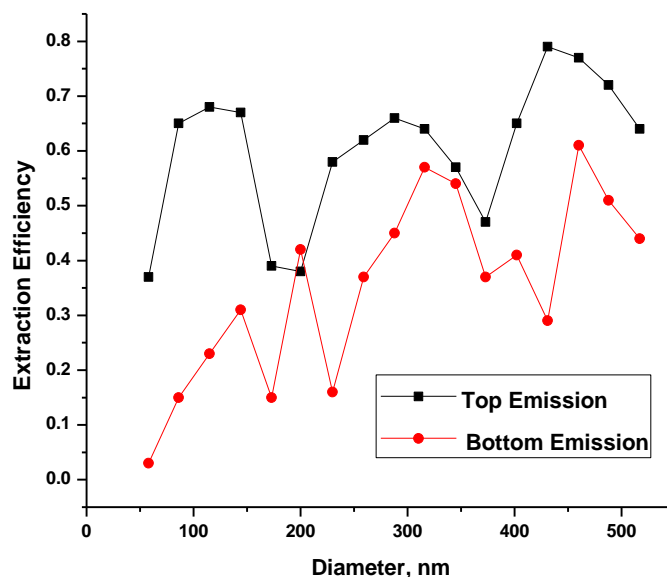


Fig 5. Extraction efficiency of nanorod LED at different diameters of nanorod.

In the FDTD simulation, a single point source polarized in the in-plane direction was positioned at the center of the InGaN MQW layers. In the simulated nanorod LED structure, light emitted from the center of rods escapes through either the sapphire substrate or the encapsulated materials above the nanorods. In the FDTD computational domain as shown in Fig 4, there are two detection planes for propagating electromagnetic waves. At the top detection plane, the LEE through the encapsulated material (top emission) and at the bottom detection plane the LEE through the sapphire substrate (bottom emission) is calculated.

In Fig. 5, the LEE for a single nanorod LED is plotted as a function of the diameter of rod. Here, the height of the nanorod is fixed at 500 nm and fill factor is fixed at 0.5. LEE is defined as the fraction of emitted power out of the LED surface to the emitted power from the MQW, which is determined by the ratio of pointing vectors integrated over the extraction surface to the integrated pointing vectors over the MQW. As shown in Fig. 5, there is a periodic behavior for both top and bottom emission of the LEE which relates the existence of resonant modes inside the nanorod. Since the nanorod structure can be regarded as a cylindrical resonant cavity, a resonant mode in the radial direction is created at specific values of the rod radius. The radial mode has a large wave vector component in the radial direction, so it cannot be guided along the nanorod and easily escapes from the rod without undergoing total internal reflection. Therefore, the emission LEE reaches its local maximum values whenever the radial mode appears inside the rod at specific rod radii. The periodicity of the rod radius for maximum efficiency is about 72 nm, roughly corresponding to $\lambda / 2\pi$, where λ is the wavelength of light in vacuum. Fig. 6 implies the pointing vector intensity distribution of planar and nanorod LEDs. This clearly shows the increased intensity distribution in nanorod LED compared to planar one.

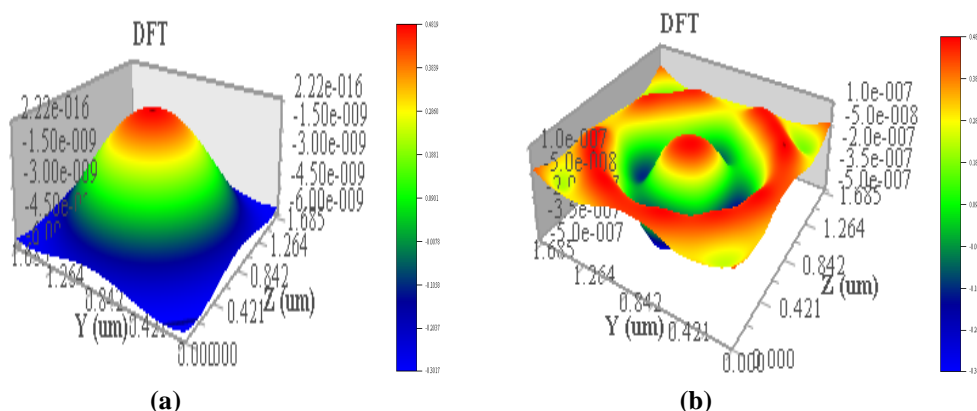


Fig. 6. FDTD simulated pointing vector intensity distribution of (a) planar and (b) nanorod LED configuration.

IV. Conclusion

Nanorod LED has also been fabricated by using self-assembled Ni nano-cluster as a mask during ICP etching. PL intensity of nanorod LED showed 2.8 times enhancement than the planar LED which reflects the enhancement of internal quantum efficiency. PL intensity emission peak blue shifted to 9nm (54meV) for nanorod LED compared to planar LED due to the suppression QCSE and strain relaxation in MQW. FDTD simulation was carried out for extraction efficiency of both top and bottom emissions of nanorod LEDs. Simulation result of nanorod LEDs showed a periodic behavior for maximum extraction efficiency with periodicity of rod radius 72nm for both top and bottom emissions. Extraction efficiency was calculated up to 80% for nanorod LEDs. Thus, nanorod LEDs is expected to be a good candidate for future LED development.

References

- [1] F. Kopp, T. Lermer, C. Eichler, U. Strauss, Cyan superluminescent light-emitting diode based on InGaN quantum wells, *Appl. Phys. Express* 5 (2012) 082105.
- [2] E. F. Schubert, *Light Emitting Diode* (Cambridge University Press, Cambridge, England, 2003).
- [3] N. Grandjean, M. Ilegems, Visible InGaN/GaN quantum-dot materials and devices, *Proceedings of the IEEE*, 95, 9 (2007).
- [4] K. P. O'Donnell, R. W. Martin, P. G. Middleton, Origin of Luminescence from InGaN Diodes, *Phys. Rev. Lett.* 82, 237 (1999).
- [5] T. Wang, J. Bai, S. Sakai, J. K. Ho, Investigation of the emission mechanism in InGaN/GaN-based light emitting diodes, *Appl. Phys. Lett.* 78, 2617-2619 (2001).
- [6] S. Chichibu, A. Uedono, T. Onuma, B. A. Haskell, A. Chakraborty, T. Koyama, P. T. Fini, S. Keller, S. P. DenBaars, J. S. Speck, U. K. Mishra, S. Nakamura, S. Yamaguchi, S. Kamiyama, H. Amano, I. Akasaki, J. Han, T. Sota, *Nature Mater.* 5, 810 (2006).
- [7] P. Gibart, Metal organic vapour phase epitaxy of GaN and lateral overgrowth, *Rep. Prog. Phys.* 67(5), 667- 715 (2004).
- [8] Y. J. Hong, C. H. Lee, A. Yoon, M. Kim, H. K. Seong, H. J. Chung, C. Sone, Y. J. Park, G. C. Yi, Visible color-tunable light-emitting diodes, *Adv. Mater.* 23(29), 3284-3288 (2011).
- [9] T. W. Yeh, Y. T. Lin, L. S. Stewart, P. D. Dapkus, R. Sarkissian, J. D. O'Brien, B. Ahn, S. R. Nutt, InGaN/GaN multiple quantum wells grown on nonpolar facets of vertical GaN nanorod arrays, *Nano Lett.* 12(6), 3257-3262 (2012).
- [10] T. Takeuchi, H. Amano, I. Akasaki, Theoretical study of orientation dependence of piezoelectric effects in wurtzite strained GaInN/GaN heterostructures and quantum wells, *Jpn. J. Appl. Phys.* 39 (Part 1, No. 2A), 413-416 (2000).
- [11] A. Waag, X. Wang, S. Fündling, J. Ledig, M. Erenburg, R. Neumann, M. A. Suleiman, S. Merzsch, J. Wei, S. Li, H. H. Wehmann, W. Bergbauer, M. Straßburg, A. Trampert, U. Jahn, H. Riechert, The nanorod approach: GaN nano LEDs for solid state lighting, *Phys. Status Solidi* 8(7-8), 2296-2301 (2011).
- [12] A. Kikuchi, M. Kawai, M. Tada, K. Kishino, InGaN/GaN multiple quantum disk nanocolumn light-emitting diodes grown on (111) Si substrate, *Japan. J. Appl. Phys.* 43, L1524-L1526 (2004).
- [13] H. M. Kim, D. S. Kim, T. W. Kang, Y. H. Cho, K. S. Chung, Growth and characterization of single-crystal GaN nanorods by hydride vapor phase epitaxy, *Appl. Phys. Lett.* 81, 2193-2195 (2002).
- [14] W. Q. Han, S. S. Fan, Q. Q. Li, Y. D. Hu, Synthesis of gallium nitride nanorods through a carbon nanotube-confined reaction *Science* 277, 1287-1289 (1997).
- [15] C. C. Yu, C. F. Chu, J. Y. Tsai, H. W. Huang, T. H. Hsueh, C. F. Lin, S. C. Wang, Gallium nitride nanorods fabricated by inductively coupled plasma reactive ion etching, *Japan. J. Appl. Phys.* 41, L910 (2002).
- [16] H. S. Chen, D. M. Yeh, Y. C. Lu, C. Y. Chen, C. F. Huang, T. Y. Tang, C. C. Yang, C. S. Wu, C. D. Chen, Strain relaxation and quantum confinement in InGaN/GaN nanoposts, *Nanotechnology* 17, 1454-1458 (2006).
- [17] H. Sekiguchi, K. Kishino, A. Kikuchi, Emission color control from blue to red with nanocolumn diameter of InGaN/GaN nanocolumn arrays grown on same substrate, *Appl. Phys. Lett.* 96(23), 231104 (2010).
- [18] T. W. Yeh, Y. T. Lin, L. S. Stewart, P. D. Dapkus, R. Sarkissian, J. D. O'Brien, B. Ahn, S. R. Nutt, InGaN/GaN multiple quantum wells grown on nonpolar facets of vertical GaN nanorod arrays, *Nano Lett.* 12(6), 3257-3262 (2012).
- [19] G. Yang, Y. Guo, H. Zhu, D. Yan, G. Li, S. Gao, K. Dong, Fabrication of nanorod InGaN/GaN multiple quantum wells with self-assembled Ni nano-island masks, *Applied Surface Science*, 285 (Part B), 772 (2013).
- [20] S. Y. Bae, D. J. Kong, J. Y. Lee, D. J. Seo, D. S. Lee, Size-controlled InGaN/GaN nanorod array fabrication and optical characterization, *Optics Express*, 21(14), 16854-16862 (2013).